# Advanced virtual monoenergetic imaging algorithm for lower extremity computed tomography angiography: effects on image quality, artifacts, and peripheral arterial disease evaluation

Jung Han Hwang

Jin Mo Kang

Suyoung Park

So Hyun Park

Jeong Ho Kim

Ki Hyun Lee

Ji Hoon Shin

Seong Yong Pak

**Jung Han Hwang and Jin Mo Kang contributed equally to this study and share the first authorship.**

**PURPOSE**

To investigate the image quality of lower extremity computed tomography angiography (LE-CTA) using a reconstruction algorithm for monoenergetic images (MEIs) to evaluate peripheral arterial disease (PAD) at different kiloelectron volt (keV) levels.

**METHODS**

A total of 146 consecutive patients who underwent LE-CTA on a dual-energy scanner to obtain MEIs at 40, 50, 60, 70, and 80 keV were included. The overall image quality, segmental image quality of the arteries and PAD segments, venous contamination, and metal artifacts from prostheses, which may compromise quality, were analyzed.

**RESULTS**

The mean overall image quality of each MEI was $2.9 \pm 0.7$, $3.6 \pm 0.6$, $3.9 \pm 0.3$, $4.0 \pm 0.2$, and $4.0 \pm 0.2$ from 40 to 80 keV, respectively. The segmental image quality gradually increased from 40 to 70–80 keV until reaching its highest value. Among 295 PAD segments in 68 patients, 40 (13.6%) were scored at 1–2 at 40 keV and 13 (4.4%) were scored at 2 at 50 keV, indicating unsatisfactory image quality due to the indistinguishability between high-contrast areas and arterial calcifications. The segments exhibiting metal artifacts and venous contamination were reduced at 70–80 keV ($2.6 \pm 1.2$, $2.7 \pm 0.5$) compared with at 40 keV ($2.4 \pm 1.1$, $2.5 \pm 0.7$).

**CONCLUSION**

The LE-CTA method using a reconstruction algorithm for MEIs at 70–80 keV can enhance the image quality for PAD evaluation and improve mitigate venous contamination and metal artifacts.

**KEYWORDS**

Artifact, atherosclerosis, computed tomography angiography, peripheral arterial disease, radiation dosage

From the Department of Radiology (J.H.H., S.P. ✉ spgir@naver.com, S.H.P., J.H.K.), Gachon University College of Medicine, Gil Medical Center, Incheon, South Korea; Department of Surgery (J.M.K.), Gachon University College of Medicine, Incheon, South Korea; Department of Radiology and Research Institute of Radiology (J.H.S.), University of Ulsan College of Medicine, Asan Medical Center, Seoul, South Korea; Department of Biomedical Engineering (S.Y.P.), University of Ulsan College of Medicine, Asan Medical Institute of Convergence Science and Technology, Asan Medical Center, Seoul, South Korea.

Peripheral arterial disease (PAD) affects older patients with atherosclerosis and is a common reason for recurrent hospital visits.[1] Lower extremity computed tomography angiography (LE-CTA) can be used to detect PAD, assess anatomic variations, determine suspected limb ischemia, carry out treatment planning, and evaluate stent placement.[2] Likewise, current guidelines recommend LE-CTA examinations to evaluate PAD, the severity of atherosclerosis, and treatment planning.[1,3,4]

Dual-energy CT can enhance both the tissue contrast in monoenergetic images (MEIs) by using reconstruction algorithms[5] and the visualization of vascular anatomy by using bone removal algorithms.[6,7] An MEI enables optimization of the kiloelectron volt (keV) level to evaluate the objective and subjective image quality of tumors, large vessels, metal artifacts, and ancillary features.[8-15] While low keV (40–50 keV) imaging provides a higher contrast than high keV (70–90 keV) imaging, the former presents more severe noise than the latter. Recently,

a noise-reduced virtual MEI reconstruction algorithm (synonym MEI plus) was developed to mitigate image noise at low energy levels.[16] In fact, this algorithm can reduce the image noise at a low keV and improve the image contrast at a high keV, even achieving the highest image contrast, effectively removing image noise at a low keV and enhancing the signal-to-noise ratio and contrast-to-noise ratio in vascular imaging.[17,18] However, to the best of our knowledge, MEI plus has not been used to optimize the keV level in LE-CTA to evaluate PAD, venous contamination, and metal artifacts. In this study, the objective and subjective image quality of MEIs obtained from LE-CTA at different keV levels after applying MEI plus are compared.

## Methods

### Patients

This study was approved by the Basic Science Research Program through the National Research Foundation of Korea and was funded by the Ministry of Science ICT and Future Planning (study number: GBIRB2020-435). Written informed consent was waived due to the retrospective nature of this study. Patients who underwent LE-CTA on a dual-energy scanner for either the evaluation or follow-up of PAD between July 2018 and December 2018 were included. The Picture Archiving and Communication Systems database was searched to collect the data of patients who met the criteria, and 157 consecutive patients were identified. The exclusion criteria included a change in examination protocol and the loss of dose reports. Following screening, 146 patients (91 men and 55 women; mean age= 64.7 ± 13.9 years; age range= 26–92 years) were enrolled in this study (Figure 1). The characteristics of the patients and radiation dose parameters are summarized in Table 1.

### Main points

- Low kiloelectron volt (keV) levels provide a higher contrast but more severe noise than high keV levels.

- Both the objective and the subjective image quality of monoenergetic images (MEIs) obtained from lower extremity computed tomography angiography at different keV levels after applying a noise-reduced virtual MEI reconstruction algorithm were compared.

- The MEIs at 70 and 80 keV levels can both enhance the image quality and mitigate image noise.

### Computed tomography examination protocol

The patients underwent LE-CTA from the T12 vertebra to the lower end of the feet following intravenous injection of 30 mL at 4 mL/s followed by 80 mL at 3 ml/s of iohexol 350 mgI/mL (Bonorex 350; Central Medical Service, Seoul, Republic of Korea). Bolus tracking was used for the imaging. A region of interest (ROI) was positioned at the aortic bifurcation with a trigger threshold of 150 Hounsfield units (HU) before CT scans were acquired using a 128-slice CT scanner (Somatom Definition Flash; Siemens Healthcare, Erlangen, Germany) in the dual-source mode at a tube voltage of 80 kVp (tube detector A; reference, 250 mAs) and 140 kVp with a tin filter (tube detector B; reference, 106 mAs)

using tube current modulation of the dose (CARE Dose 4D; Siemens Healthcare). The images were reconstructed by applying a blending factor of 0.4 (M_0.4; 40% of 80 kVp and 60% of 140 kVp with a tin filter spectrum). The MEIs with a (axial) slice thickness of 5 mm acquired at 40, 50, 60, 70, and 80 keV were reconstructed on a multimodality workstation (Syngo.via VB20; Siemens Healthcare).

### Qualitative analysis

The MEIs were independently reviewed with blinded patient information in consensus by two interventional radiologists (S.P. and J.H.H.), who had nine and 12 years of experience, respectively, at the time of the study. Any discrepancies were resolved by
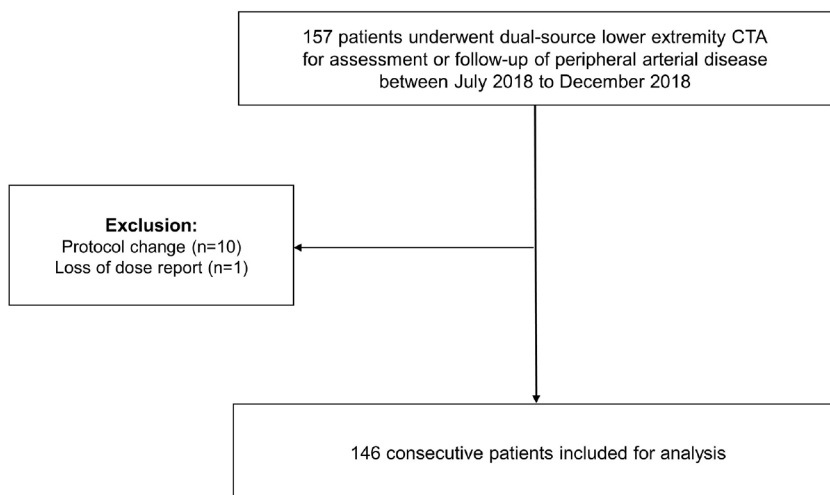


Figure 1. Study flowchart.

**Table 1.** Patient characteristics and radiation dose parameters

| Parameter | All patients (n = 146) |
|---|---|
| Demographics | |
| Male[a] | 91 (62.3) |
| Female[a] | 55 (37.7) |
| Age (years)[b] | 64.7 ± 13.9 (26–92) |
| Height (cm)[b] | 162.6 ± 9.9 (140–183) |
| Weight (kg)[b] | 61.5 ± 12.2 (36.7–96) |
| BMI (kg/m²)[b] | 23.2 ± 4.8 (13.6–40.7) |
| Medical history of patients | |
| Diabetes[a] | 53 (36.3) |
| Hypertension[a] | 66 (45.2) |
| Cardiovascular disease[a] | 31 (21.2) |
| Chronic kidney disease[a] | 20 (13.7) |
| CT angiography parameters | |
| CTDI$_{vol}$ (mGy)[b] | 7.6 ± 0.5 (6.9–9.7) |
| Dose-length product (mGy-cm)[b] | 970.3 ± 112.9 (711–1357) |

[a]Data are number of patients (percentages); [b]data are means ± standard deviations (ranges). BMI, body mass index; CT, computed tomography; CTDI, CT volume dose index.

consensus. The overall image quality of the CT scans and the segmental image quality of infrarenal abdominal aorta, common iliac arteries (CIAs), external iliac arteries (EIAs), common femoral arteries (CFAs), superficial femoral arteries (SFAs), popliteal arteries (PAs), anterior tibial arteries (ATAs), posterior tibial arteries (PTAs), peroneal arteries, and tibioperoneal trunk (TPT) were scored using a four-point scale,[5,11] where scores of 0 and 1 were considered as unacceptable for vessel assessment. Venous contamination was scored using a three-point scale. The presence of stenosis and/or occlusion of LE arteries was evaluated, and the degree of stenosis was graded in terms of mild, moderate, and severe.[12] Then, the diagnostic value in terms of prosthesis artifacts was scored using a four-point scale (Table 2).

### Quantitative analysis

For comparative analysis, one blinded radiologist established a circular ROI with a size of 1–3 cm$^2$ at specific levels of axial images from the five image sets at different keV levels. The levels were the infrarenal abdominal aorta and the midportion of the bilateral CIAs. The mean attenuation and standard deviation (i.e. noise) of HU in the ROI were calculated.

### Radiation dose

The CT volume dose index [CTDI$_{vol}$ in milligrays (mGy)] and dose-length product (DLP in mGy·cm) were used to estimate the radiation dose from the dose report of the CT scan.

### Statistical analysis

The quantitative image analysis was compared among the five image sets using the analysis of variance method and adjustment with Bonferroni correction for multiple comparisons, with a $P$ value of <0.01 regarded as significant. Interobserver agreement regarding the overall image quality on LE-CTA was determined using kappa statistics with the following scales: 0.01–0.20, slight agreement; 0.21–0.40, fair; 0.41–0.60, moderate; 0.61–0.80, substantial; and 0.81–1.00, excellent. All statistical analyses were performed using SPSS statistical software (version 25.0; IBM, Armonk, NY, USA).

## Results

Among the 146 patients, 68 (46.6%) presented PAD in 295 image segment of arteries in the LE-CTA examinations. The arteries with PAD included 12 CIAs, two CFAs, five
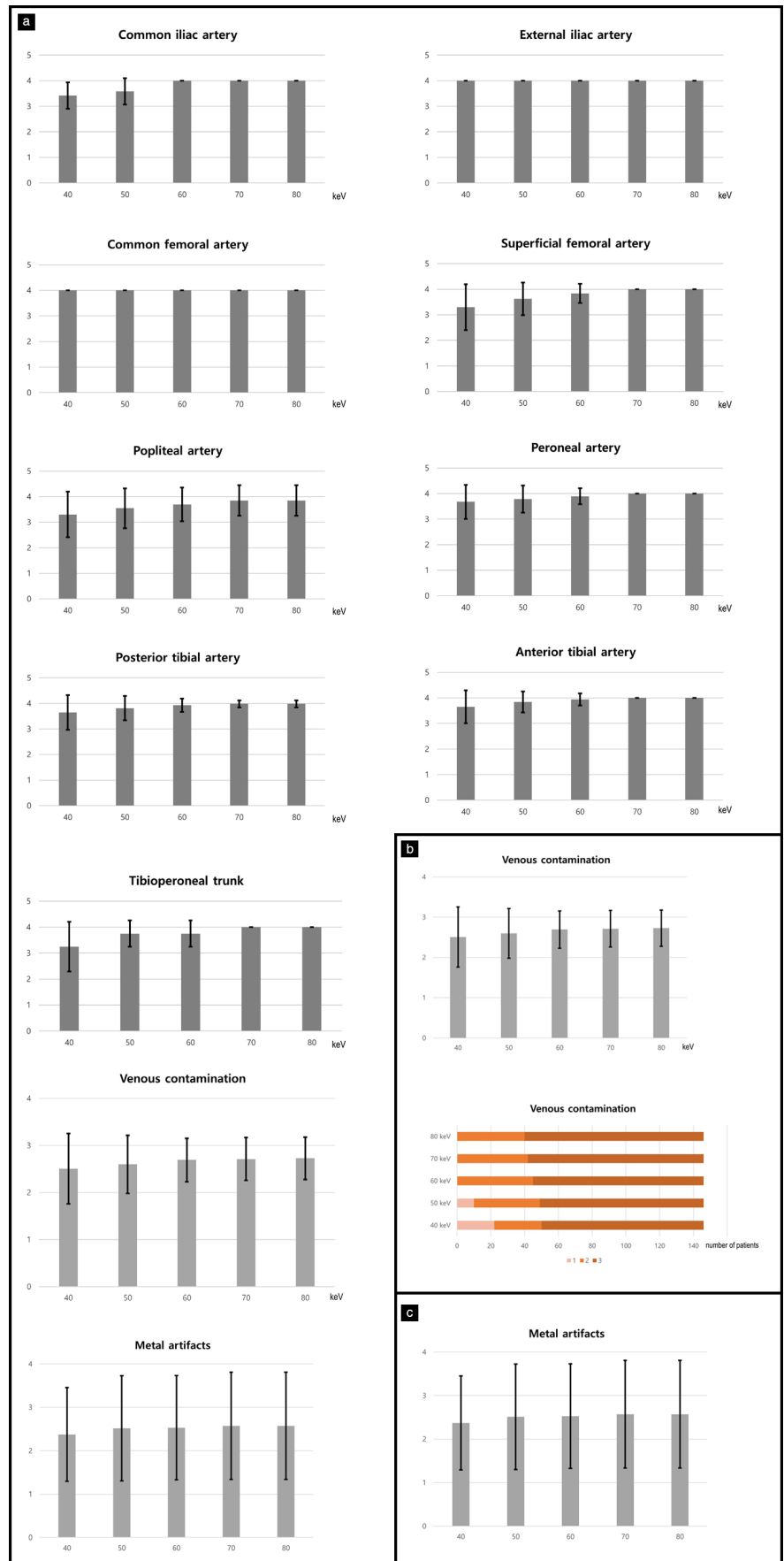


Figure 2. (a-c) Mean (bar graphs) and standard deviation (error bar) of the subjective image quality scores from segmental arteries, venous contamination, and metal artifacts at different keV levels. keV, kiloelectron volt.

EIAs, 61 SFAs, 68 ATAs, 54 PTAs, 37 peroneal arteries, 46 PAs, and 10 TPT branches. The LE-CTA examinations of 14 patients revealed 15 segments with stent placement (eight patent stents and seven in-stent restenosis). In addition, 33 patients presented 77 segments (three right CIAs, three left CIAs, one right EIA, one left EIA, four right CFAs, one left CFA, six right SFAs, 10 left SFAs, 16 right PAs, 17 left PAs, five right ATAs, five left ATAs, one right peroneal artery, one left peroneal artery, one right PTA, and two left PTAs) containing metal artifacts of prostheses [14 right total knee replacements (TKRs), 13 left TKRs, seven right leg internal fixations (IFs), 11 left leg IFs, two pelvic bone IFs, two posterior lumbar IFs, three right total hip replacements (THRs), one left THR, and one left leg external fixation], all of which may compromise the LE-CTA image quality of the arteries.

The overall quality of the 40, 50, 60, 70, and 80 keV MEIs was 2.9 ± 0.7 (range: 2–4), 3.6 ± 0.6 (range: 2–4), 3.9 ± 0.3 (range: 3–4), 4.0 ± 0.2 (range: 3–4), and 4.0 ± 0.2 (range: 3–4), respectively. All pairwise comparisons, except the 60 vs. 70 vs. 80 keV MEIs, were sig-nificantly different ($P < 0.001$). Interobserver agreement was excellent for the overall image quality (kappa: 0.89).

The subjective segmental image quality significantly increased in the CIA, SFA, PA, peroneal artery, ATA, PTA, and TPT MEIs at 70 and 80 keV compared with lower keV levels (Figure 2). The segmental image quality gradually increased from 40 to 70–80 keV, reaching its highest value at 70 and 80 keV. Among the 295 PAD segments, 40 (13.6%) were scored at 1–2 at 40 keV (score 1, 2 segments; score 2, 38 segments) and 13 (4.4%) were scored at 2 at 50 keV, indicating unsatisfactory image quality due to the indistinguishability between high-contrast areas and arterial calcifications (Figure 3). Meanwhile, 199 (67.5%) of the 295 PAD segments were scored at 4 at 40–80 keV.

Among the 75 segments exhibiting occlusion, 68 (90.7%) were equally scored from 40 to 80 keV. The attenuation and noise of the objective segmental image quality gradually decreased from 40 to 80 keV (Table 3). All pairwise comparisons for attenuation indicated a significant difference ($P < 0.01$). The pairwise comparison for noise, 70 vs. 80 ($P$ = 1.000) keV MEI on right CIA, 60 vs. 70 ($P$ = 0.565), 60 vs. 80 ($P$ = 0.014), and 70 vs. 80 ($P$ = 1.000) keV MEI on the left CIA, indicated a difference without significance, while further pairwise comparisons of noise for infrarenal abdominal aorta and bilateral CIAs indicated a significant difference ($P < 0.01$) (Table 4).

The score of segments exhibiting metal artifacts slightly increased from 40 (2.4 ± 1.1) to 70–80 keV (2.6 ± 1.2). Among the 77 segments exhibiting metal artifacts, 63 (81.8%) were identically scored from 40 to 80 keV (score 1: 21 segments; score 2: 12 segments; score 3: 16 segments; score 4: 14 segments). In addition, 22 segments were scored at 1 (non-diagnostic image quality) at 40–50 keV, and 21 segments were scored at 1 at 60–80 keV (Figure 4). Most score differences (10/14 segments) were scored at 3 (slight artifacts) or 4 (excellent image quality) at 40–50 keV compared with the imaging at 60–80 keV.

The score of segments exhibiting venous contamination slightly increased from 40 (2.5 ± 0.7) to 70–80 keV (2.7 ± 0.5). The pairwise comparison, 40 vs. 80 ($P$ = 0.008) keV MEI, indicated a significant difference in terms of noise for venous contamination, while further corresponding pairwise comparisons, at 40 vs. 60 ($P$ = 0.048), 40 vs. 70 ($P$ = 0.017), 50 vs. 80 ($P$ = 0.467) keV MEI, indicated a difference without significance. Among the 146 patients, 22 (15.1%) exhibited segments with a score of 1 (visible and compromises diagnostic interpretation) in venous contamination at 40 keV, and 10 (6.8%) exhibited segments with a score of 1 at 50 keV in the LE-CTA examinations, while no imaging results were scored 1 at 60–80 keV.

## Discussion

In this study, the image quality of MEIs acquired at five keV levels in terms of PAD, venous contamination, and metal artifacts were compared to determine the MEI acquisition with the highest image quality. The subjective image quality in segments exhibiting PAD at 70–80 keV was higher than that at 40–60 keV. The venous contamination and metal artifacts were more decreased in the MEIs at 70–80 keV than those at 40–60 keV. In addition, the diagnostic interpretation of 22 and 10 patients was compromised due to venous contamination in the MEIs at 40 and 50 keV, respectively, while venous contamination did not affect the diagnostic interpretation of the MEIs at 60–80 keV. Therefore, MEIs with a low keV level may lead to degraded subjective image quality for PAD evaluation, despite the high contrast.

---

**Table 2.** Subjective image analysis and evaluation of PAD

**1. Subjective image analysis**

  **a)** Overall CT image quality

  **b)** Segmented image quality of infrarenal aorta, CIA, EIA, CFA, SFA, PA, ATA, PTA, peroneal artery, and TPT

    1: If examination did not provide information for diagnosis

    2: If examination maintained acceptable information but unsatisfactory image quality

    3: If examination was satisfactory to provide information with adequate image quality

    4: If examination provided optimal information with excellent image quality

  **c)** Venous contamination

    1: Visible and compromises diagnostic interpretation

    2: Visible, not affect diagnostic interpretation

    3: Not visible

**2. Peripheral arterial disease and artifact evaluation**

  **a)** Peripheral arterial disease

    Stenosis, 1: mild, decreased luminal diameter below 1/3

    Stenosis, 2: moderate, decreased luminal diameter 1/3–2/3

    Stenosis, 3: severe, decreased luminal diameter above 2/3

    Occlusion

  **b)** Diagnostic value in artifact of prosthesis

    1: Non-diagnostic image quality, strong streak artifacts, insufficient quality for diagnostic purposes

    2: Severe artifacts causing uncertainty

    3: Slight artifacts with adequate diagnostic image evaluation

    4: Excellent image quality, no artifacts

PAD, peripheral arterial disease; CT, computed tomography; CIA, common iliac artery; EIA, external iliac arteries; CFA, common femoral arteries; SFA, superficial femoral artery; PA, popliteal artery; ATA, anterior tibial artery; PTA, posterior tibial arteries; TPT, tibioperoneal trunk.
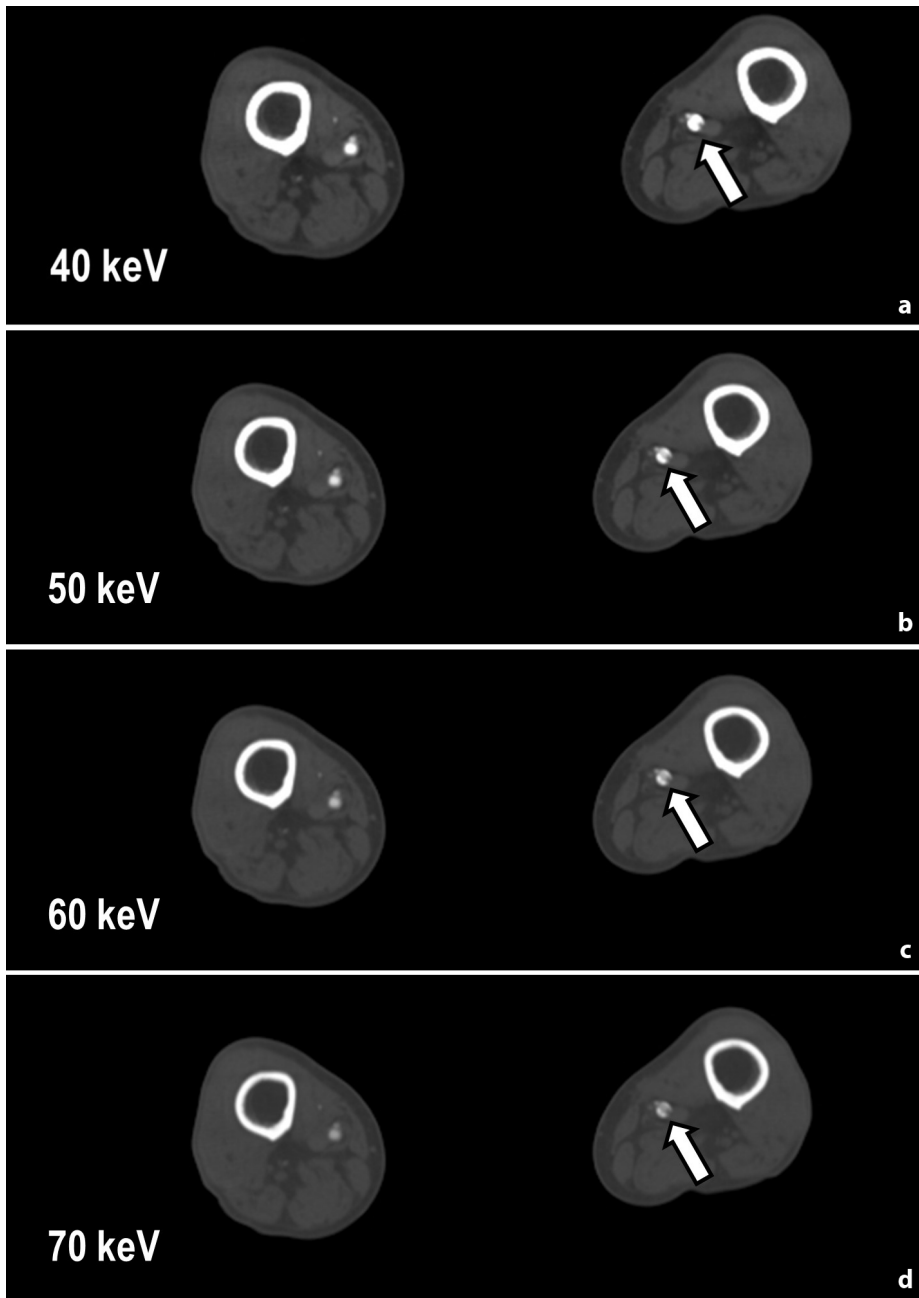
**Figure 3. (a-d)** The LE-CTA using MEI plus in a 71-year-old man with PAD (body mass index: 21.9 kg/m$^2$; CTDIvol: 7.1 mGy; DLP: 936 mGy·cm). The patient presented grade 3 stenosis from left SFA (arrowhead) to PA. The 40–50 and 60 keV MEIs were scored 2 and 3, respectively, in terms of diagnostic value in segmental image quality in the left PA. Unsatisfactory image quality was observed for vascular calcification at 40–50 keV, but optimal image quality was achieved at 70–80 keV (score 4). LE-CTA, lower extremity computed tomography angiography; MEIs, monoenergetic images; PAD, peripheral arterial disease; CTDI, CT volume dose index; DLP, dose-length product; SFA, superficial femoral artery; PA, popliteal arteries; keV, kiloelectron volt.

Several studies have reported that the image quality of high-keV (70–100 keV) MEIs is superior for calcific or noncalcified plaque in arterial disease[8,19] and for metal artifacts[9,20,21] compared with low-keV (40–50 keV) MEIs, regardless of the use of noise optimizing methods (e.g., MEI plus algorithm). These findings are consistent with the highest subjective image quality achieved at 70–80 keV for the evaluation of PAD and metal artifacts in our study. Symons et al.[8] reported low-keV images yielding significantly higher arterial plaque volumes than conventional 90/Sn150-kVp images. Likewise, unsatisfactory image quality was observed in 13.6% PAD segments at 40 keV and 4.4% PAD segments at 50 keV in our study. While small high-contrast structures with blooming artifacts can be mitigated by optimizing the window length/window width,[22,23] low-keV images

with a high contrast can lead to misinterpretation or overestimation of PAD calcification. Therefore, it may not be appropriate to perform PAD evaluation using low-keV MEIs, even if using reconstruction algorithms such as MEI plus.

Beeres et al.[24] reported that MEI plus at a low keV (40–50 keV) provides low image noise in aortic segments, which is not consistent with our results. This difference may be attributed to their evaluation of the aorta (the largest vessel) and their neglection of small vessels, PAD, and metal artifacts. Moreover, their results indicated lower noise at a low keV using MEI plus compared with MEI alone. Our study focused on the image quality of peripheral vessels at low and high keV levels using MEI plus in both cases. Here, low keV levels provided higher objective image noise and lower subjective image quality for PAD, venous contamination, and metal artifacts than high keV levels. We expect our results to be more consistent with clinical practice when evaluating PAD using LE-CTA.

Severe venous contamination was observed in the MEIs from 15.1% of the patients at 40 keV and from 6.8% of the patients at 50 keV, while no compromise in diagnostic interpretation due to venous contamination was determined at 60–80 keV, suggesting another disadvantage of low-keV MEIs. Furthermore, while low-keV MEIs provide a high contrast, this can lead to the overestimation of small venous contamination. While venous contamination at a low keV can be reduced by the optimization of the window settings, venous contamination may also adversely affect LE-CTA at low keV levels.

This study involves certain limitations. First, the images from a small number of patients exhibited stent placement on the evaluated artery segments. Given that stents may also cause artifacts and might reduce the image quality, optimizing the keV level for evaluation of stent patency and in-stent restenosis should be conducted by including more patients with arterial stents. Second, the CT image sets were acquired from a single scanner, and the results may be neither generalizable nor directly comparable with those obtained from other scanners. Third, since the results were not compared to those of catheter angiography, which is the reference standard, the diagnostic accuracy of CTA was not sufficiently evaluated. Fourth, interobserver agreement was not evaluated, except in terms of the overall image quality since the analyses were conducted using the consensus reading method. Finally, the

**Table 3.** Quantitative analysis of MEI attenuation and noise in five image sets

| Parameter (keV) | 40 | 50 | 60 | 70 | 80 |
|---|---|---|---|---|---|
| Quantitative analysis (Hounsfield unit) | | | | | |
| Attenuation | | | | | |
| Infrarenal aorta | 1547.2 ± 348.9 | 1031.2 ± 233.3 | 725.8 ± 162.8 | 526.1 ± 115.6 | 427.6 ± 290.2 |
| Right CIA | 1513.9 ± 349.5 | 1021.0 ± 235.6 | 753.8 ± 162.0 | 541.9 ± 119.9 | 421.4 ± 91.5 |
| Left CIA | 1522.4 ± 341.0 | 1027.2 ± 228.8 | 724.6 ± 160.5 | 540.4 ± 119.4 | 416.9 ± 91.0 |
| Noise | | | | | |
| Infrarenal aorta | 46.5 ± 14.6 | 31.0 ± 9.9 | 21.6 ± 6.9 | 16.3 ± 7.8 | 12.3 ± 3.7 |
| Right CIA | 47.2 ± 34.3 | 32.3 ± 24.4 | 22.9 ± 18.2 | 17.4 ± 14.4 | 14.3 ± 11.9 |
| Left CIA | 46.8 ± 29.1 | 34.8 ± 38.3 | 23.8 ± 18.8 | 18.2 ± 15.0 | 14.5 ± 12.3 |

Data shown are mean ± standard deviation. MEIs, monoenergetic images; keV, kiloelectron volt; CIA, common iliac artery.
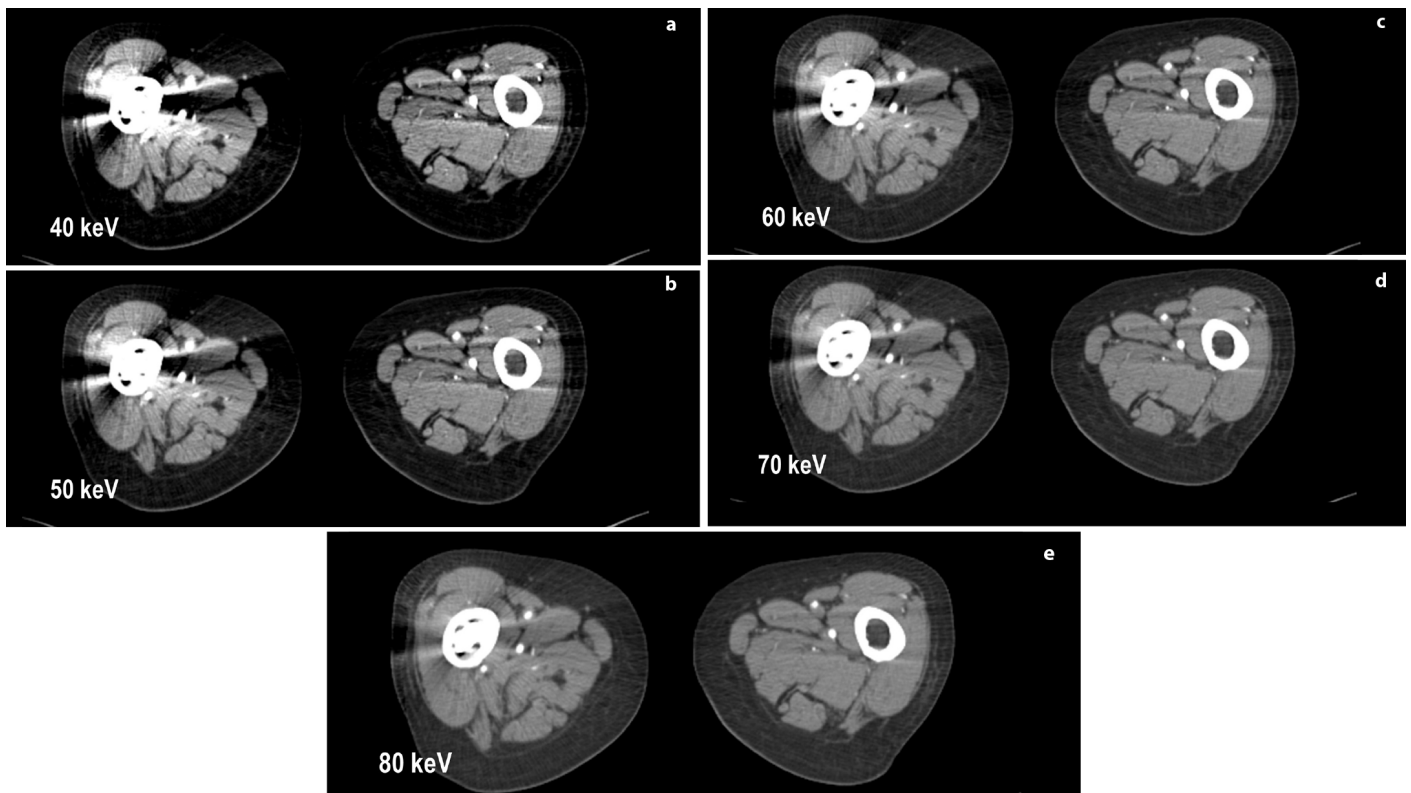


**Figure 4. (a-e)** The LE-CTA using MEI plus in an 80-year-old woman (body mass index: 23.8 kg/m$^2$; CTDIvol: 7.8 mGy; DLP: 956 mGy·cm) with PAD in both SFAs, both PAs, and both PTAs as well as grade 3 stenosis. Metal artifacts caused by total hip replacement affect the right SFA evaluation, and their effect gradually decreases in images from 40 to 80 keV. The diagnostic value scores of segmented image quality were 1, 2, 3 and 4 at 40, 50, 60–70, and 80 keV, respectively. LE-CTA, lower extremity computed tomography angiography; MEIs, monoenergetic images; CTDI, CT volume dose index; DLP, dose-length product; PAD, peripheral arterial disease; SFA, superficial femoral artery; keV, kiloelectron volt.

**Table 4.** Quantitative analysis of MEI attenuation and noise in five image sets (*P* values)

| Parameter (keV) | | | Noise | | | Attenuation | | |
|---|---|---|---|---|---|---|---|---|
| | | | Ao | RCIA | LCIA | Ao | RCIA | LCIA |
| 40 | | vs. 50 | <0.001 | <0.001 | <0.001 | <0.001 | <0.001 | <0.001 |
| | | vs. 60 | <0.001 | <0.001 | <0.001 | <0.001 | <0.001 | <0.001 |
| | | vs. 70 | <0.001 | <0.001 | <0.001 | <0.001 | <0.001 | <0.001 |
| | | vs. 80 | <0.001 | <0.001 | <0.001 | <0.001 | <0.001 | <0.001 |
| 50 | | vs. 60 | <0.001 | 0.003 | 0.002 | <0.001 | <0.001 | <0.001 |
| | | vs. 70 | <0.001 | <0.001 | <0.001 | <0.001 | <0.001 | <0.001 |
| | | vs. 80 | <0.001 | <0.001 | <0.001 | <0.001 | <0.001 | <0.001 |
| 60 | | vs. 70 | <0.001 | 0.320* | 0.565* | <0.001 | <0.001 | <0.001 |
| | | vs. 80 | <0.001 | 0.009 | 0.014* | <0.001 | <0.001 | <0.001 |
| 70 | | vs. 80 | 0.003 | >0.999* | > 0.999* | 0.006 | <0.001 | <0.001 |

*Not statistically significant (*P* ≥ 0.01). MEIs, monoenergetic images; keV, kiloelectron volt; Ao, infrarenal aorta; RCIA, right common iliac artery; LCIA, left common iliac artery.

data corresponding to a level of >90 keV, MEIs with polyenergetic images, or other MEI blending factors were not compared. Further studies including polyenergetic images and various combinations of MEIs should be conducted.

In conclusion, among the MEIs at different keV levels, the 70–80 keV MEIs obtained higher diagnostic interpretation scores in the overall and segmental subjective image quality evaluations that also considered metal artifacts. The image quality at 60–80 keV was more acceptable in terms of venous contamination since the higher contrast in low-keV images may lead to the overestimation of small venous contamination.

### Conflict of interest disclosure

The authors declared no conflicts of interest.

## References

1. Fowkes FG, Rudan D, Rudan I, et al. Comparison of global estimates of prevalence and risk factors for peripheral artery disease in 2000 and 2010: a systematic review and analysis. *Lancet*. 2013;382(9901):1329-1340. [CrossRef]

2. Horehledova B, Mihl C, Milanese G, et al. CT Angiography in the lower extremity peripheral artery disease feasibility of an ultra-low volume contrast media protocol. *Cardiovasc Intervent Radiol*. 2018;41(11):1751-1764.

3. Aboyans V, Ricco JB, Bartelink MEL, et al. 2017 ESC Guidelines on the Diagnosis and Treatment of Peripheral Arterial Diseases, in collaboration with the European Society for Vascular Surgery (ESVS): document covering atherosclerotic disease of extracranial carotid and vertebral, mesenteric, renal, upper and lower extremity arteriesEndorsed by: the European Stroke Organization (ESO) The Task Force for the Diagnosis and Treatment of Peripheral Arterial Diseases of the European Society of Cardiology (ESC) and of the European Society for Vascular Surgery (ESVS). *Eur Heart J*. 2018;39(9):763-816. [CrossRef]

4. Criqui MH, Aboyans V. Epidemiology of peripheral artery disease. *Circ Res*. 2015;116(9):1509-1526. [CrossRef]

5. May MS, Wiesmueller M, Heiss R, et al. Comparison of dual- and single-source dual-energy CT in head and neck imaging. *Eur Radiol*. 2019;29(8):4207-4214. [CrossRef]

6. Yamamoto S, McWilliams J, Arellano C, et al. Dual-energy CT angiography of pelvic and lower extremity arteries: dual-energy bone subtraction versus manual bone subtraction. *Clin Radiol*. 2009;64(11):1088-1096. [CrossRef]

7. Sommer WH, Johnson TR, Becker CR, et al. The value of dual-energy bone removal in maximum intensity projections of lower extremity computed tomography angiography. *Invest Radiol*. 2009;44(5):285-292. [CrossRef]

8. Symons R, Choi Y, Cork TE, et al. Optimized energy of spectral coronary CT angiography for coronary plaque detection and quantification. *J Cardiovasc Comput Tomogr*. 2018;12(2):108-114. [CrossRef]

9. Mocanu I, Van Wettere M, Absil J, Bruneau M, Lubicz B, Sadeghi N. Value of dual-energy CT angiography in patients with treated intracranial aneurysms. *Neuroradiology*. 2018;60(12):1287-1295. [CrossRef]

10. Albrecht MH, Vogl TJ, Martin SS, et al. Review of clinical applications for virtual monoenergetic dual-energy CT. *Radiology*. 2019;293(2):260-271. [CrossRef]

11. Horat L, Hamie MQ, Huber FA, Guggenberger R. Optimization of monoenergetic extrapolations in dual-energy ct for metal artifact reduction in different body regions and orthopedic implants. *Acad Radiol*. 2019;26(5):67-74. [CrossRef]

12. McNamara MM, Little MD, Alexander LF, Carroll LV, Beasley TM, Morgan DE. Multireader evaluation of lesion conspicuity in small pancreatic adenocarcinomas: complimentary value of iodine material density and low keV simulated monoenergetic images using multiphasic rapid kVp-switching dual energy CT. *Abdom Imaging*. 2015;40(5):1230-1240. [CrossRef]

13. Patino M, Prochowski A, Agrawal MD, et al. Material Separation Using Dual-Energy CT: current and emerging applications. *Radiographics*. 2016;36(4):1087-1105. [CrossRef]

14. Shinohara Y, Sakamoto M, Iwata N, et al. Usefulness of monochromatic imaging with metal artifact reduction software for computed tomography angiography after intracranial aneurysm coil embolization. *Acta Radiol*. 2014;55(8):1015-1023. [CrossRef]

15. Sudarski S, Apfaltrer P, Nance JW Jr, et al. Optimization of keV-settings in abdominal and lower extremity dual-source dual-energy CT angiography determined with virtual monoenergetic imaging. *Eur J Radiol*. 2013;82(10):574-581. [CrossRef]

16. Grant KL, Flohr TG, Krauss B, Sedlmair M, Thomas C, Schmidt B. Assessment of an advanced image-based technique to calculate virtual monoenergetic computed tomographic images from a dual-energy examination to improve contrast-to-noise ratio in examinations using iodinated contrast media. *Invest Radiol*. 2014;49(9):586-592. [CrossRef]

17. Albrecht MH, Scholtz JE, Hüsers K, et al. Advanced image-based virtual monoenergetic dual-energy CT angiography of the abdomen: optimization of kiloelectron volt settings to improve image contrast. *Eur Radiol*. 2016;26(6):1863-1870. [CrossRef]

18. Zhao L, Li F, Zhang Z, et al. Assessment of an advanced virtual monoenergetic reconstruction technique in cerebral and cervical angiography with third-generation dual-source CT: Feasibility of using low-concentration contrast medium. *Eur Radiol*. 2018;28(10):4379-4388. [CrossRef]

19. Al-Baldawi Y, Große Hokamp N, Haneder S, et al. Virtual mono-energetic images and iterative image reconstruction: abdominal vessel imaging in the era of spectral detector CT. *Clin Radiol*. 2020;75(8):641. [CrossRef]

20. Magarelli N, De Santis V, Marziali G, et al. Application and advantages of

monoenergetic reconstruction images for the reduction of metallic artifacts using dual-energy CT in knee and hip prostheses. *Radiol Med*. 2018;123(8):593-600. [CrossRef]

21. Pagniez J, Legrand L, Khung S, et al. Metal artifact reduction on chest computed tomography examinations: comparison of the iterative metallic artefact reduction algorithm and the monoenergetic approach. *J Comput Assist Tomogr*. 2017;41(3):446-454. [CrossRef]

22. Pollak AW, Norton PT, Kramer CM. Multimodality imaging of lower extremity peripheral arterial disease: current role and future directions. *Circ Cardiovasc Imaging*. 2012;5(6):797-807. [CrossRef]

23. Lee KH, Shim YS, Park SH, et al. Comparison of standard-dose and half-dose dual-source abdominopelvic CT scans for evaluation of acute abdominal pain. *Acta Radiol*. 2019;60(8):946-954. [CrossRef]

24. Beeres M, Trommer J, Frellesen C, et al. Evaluation of different keV-settings in dual-energy CT angiography of the aorta using advanced image-based virtual monoenergetic imaging. *Int J Cardiovasc Imaging*. 2016;32(1):137-144. [CrossRef]